



## Molecular Crystals and Liquid Crystals Science and Technology. Section A. Molecular Crystals and Liquid Crystals

Publication details, including instructions for authors and  
subscription information:

<http://www.tandfonline.com/loi/gmcl19>

### Interaction Between Ionophores and Biomimetic Membranes

C. Betrencourt<sup>a</sup>, A. Hochapfel<sup>a</sup>, H. Hasmonay<sup>a</sup>, P. Peretti<sup>a</sup>, M.  
Ollivon<sup>b</sup> & C. Grabielle-madelmont<sup>b</sup>

<sup>a</sup> Groupe de Recherche en Physique et Biophysique, Université Paris  
V 45, rue des Saints Pères, 75270, Paris, France

<sup>b</sup> Equipe "Physico-Chimie des Systèmes Polyphasés", URA CNRS  
1218 Université Paris-Sud, 5, rue Jean-Baptiste Clément, 92296,  
Châtenay, Malabry, France

Version of record first published: 23 Sep 2006.

To cite this article: C. Betrencourt , A. Hochapfel , H. Hasmonay , P. Peretti , M. Ollivon & C.  
Grabielle-madelmont (1995): Interaction Between Ionophores and Biomimetic Membranes, Molecular  
Crystals and Liquid Crystals Science and Technology. Section A. Molecular Crystals and Liquid Crystals,  
262:1, 179-190

To link to this article: <http://dx.doi.org/10.1080/10587259508033524>

PLEASE SCROLL DOWN FOR ARTICLE

Full terms and conditions of use: <http://www.tandfonline.com/page/terms-and-conditions>

This article may be used for research, teaching, and private study purposes. Any  
substantial or systematic reproduction, redistribution, reselling, loan, sub-licensing,  
systematic supply, or distribution in any form to anyone is expressly forbidden.

The publisher does not give any warranty express or implied or make any representation  
that the contents will be complete or accurate or up to date. The accuracy of any  
instructions, formulae, and drug doses should be independently verified with primary  
sources. The publisher shall not be liable for any loss, actions, claims, proceedings,  
demand, or costs or damages whatsoever or howsoever caused arising directly or  
indirectly in connection with or arising out of the use of this material.

## **INTERACTION BETWEEN IONOPHORES AND BIOMIMETIC MEMBRANES**

**C. BETRENCOURT, A. HOCHAPFEL, H. HASMONAY, P. PERETTI**

Groupe de Recherche en Physique et Biophysique, Université Paris V  
45, rue des Saints Pères, 75270 Paris, France

**M. OLLIVON, C. GRABIELLE-MADELMONT**

Equipe "Physico-Chimie des Systèmes Polyphasés" URA CNRS 1218  
Université Paris-Sud, 5, rue Jean-Baptiste Clément, 92296 Châtenay Malabry,  
France

### **ABSTRACT**

Insertion properties of Lasalocid and Monensin as sodium salts (LAS-Na, MON-Na) in model membranes of dipalmitoylphosphatidylcholine (DPPC) have been studied in two biomimetic buffered systems: monolayers (Langmuir Film Balance) and multilamellar bilayers (Differential Scanning Calorimetry). Effects varying with the concentration and with the surface pressure have been observed within the experimental range of molar ratios  $r = \text{antibiotic} / \text{lipid}$  from 0.005 to 0.1. The area occupied by each antibiotic molecule and the relative molecular area increase at a given pressure, are different for the two molecules. The calorimetric measurements result in concentration dependent modifications of the characteristics of the gel-liquid crystal phase transition in the case of LAS-Na. No such modifications are observed in the case of MON-Na.

### **INTRODUCTION**

Ion transport in the membrane mediated by crown ether derivatives has been subject to much interest in the literature <sup>1,2</sup>. Lasalocid and Monensin, monocarboxylic polyethers from *streptomyces*, are related to such ionophores. It is well known that they form liposoluble cation complexes by ring closure between their end groups via hydrogen bonds <sup>3,4</sup>. Such complexes are formed at the interface between lipid and water and they are driven across the bilayer by gradients in cation concentration or pH <sup>5,6</sup>.

One difference between the two ionophores is seen from their transport selectivity, since Lasalocid is most efficient for carrying  $K^+$  ions and Monensin for  $Na^+$  ions <sup>7</sup>. The antibiotic activity of these molecules probably arises from the carrier mechanism <sup>8</sup>. The compounds are used for this reason in veterinary medicine. Their efficiency in MDR (multi drug resistance) in cancer therapy was discovered recently <sup>9</sup>. This stresses the utility of further research on their action mode in the membrane.

The present investigation deals with insertion properties of Lasalocid and Monensin in biomimetic systems. The main objective of the study has been to correlate the results from monolayers and multibilayers. Dipalmitoylphosphatidylcholine has been used as lipid component. The experiments have been performed at physiological buffer concentrations in order to mimic the membrane conditions as closely as possible and the molar ratios antibiotic/lipid have been kept at low values above the limits of detectable effects.

The monolayers representing one half of the biomembrane have been obtained by Langmuir films. The influence of the antibiotic molecules on the lipid monolayer, measured from the compression isotherms, is the result of effects at the membrane interface<sup>10</sup>. This study is an extension of previous works on antibiotic/lipid mixed monolayers on pure water <sup>11,12</sup>.

The lyotropic multibilayers have been studied by Differential Scanning Calorimetry (DSC). By means of this method, modifications of the thermodynamic parameters of the gel-liquid crystal phase transition in presence of the antibiotic molecules, due to interactions with the lipid, have been studied. The first results concerning the antibiotic influence on transition temperature and enthalpy are presented.

## **EXPERIMENTAL PART**

The antibiotics as sodium salts were purchased from Sigma Chimie. Lasalocid (LAS-Na) was recrystallized from aqueous methanol and acetone, m.p. 169-172°C. Monensin (MON-Na) was recrystallized from aqueous methanol and diethoxyde, m.p. 260-264°C. Dipalmitoylphosphatidylcholine (DPPC) was of the purest available quality from Sigma Chimie.

Stock solutions of antibiotic or DPPC,  $5 \cdot 10^{-4}$  M, were prepared in chloroform-hexane 2:3 v/v and spread, mixed or separately, in the wanted molar ratios. The solvents were of analytical grade from Prolabo. They were distilled on molecular sieve for moisture removal.

The monolayers were spread at a temperature of 22°C on to a subphase of buffer Hepes 10 mM, sodium chloride 145 mM, pH 7.4. The compounds were purchased from

Sigma and the subphase solution was prepared in water treated on an Elgastat UHQ 2 system. The films were spread with a Hamilton CR-700-200 syringe (50  $\mu$ l corresponding to 1 nm<sup>2</sup> molecule<sup>-1</sup> at 150 cm<sup>2</sup>). The isotherms were measured with a Krüss film balance using a pendulum 100 and recorded with an IBM-AT computer. The compressions were performed at a speed of 0.15 nm<sup>2</sup> min<sup>-1</sup>.

For the calorimetric measurements, the lipid films (DPPC alone or with appropriate amounts of antibiotic) were resuspended at 75 mM in the Hepes buffer solution. The suspensions were vortexed twice for 3 minutes at 48°C and then sonicated in a low power sonifier (60 W) of bath type in order to promote the formation of multilamellar bilayers.

Differential Scanning Calorimetry was performed with a Perkin Elmer DSC4 instrument. The samples (~10 mg) were sealed in 40  $\mu$ l aluminium pans (Perkin Elmer Model B 014-3021) and were analysed at a heating rate of 4 deg/min in the temperature range of 5-50°C. The instrument was calibrated using lauric acid as standard.

Repeated heating scans were performed three times at least and gave reproducible results. Transition temperatures  $T$  were taken at the onset of the transition<sup>13</sup> and the  $\Delta H$  was calculated from the peak area with a computer using TADS Software. The stability of the samples was controlled by DSC recording after two weeks of storage at 4°C. No significant modifications of the thermodynamic parameters were observed in these conditions.

## **RESULTS AND DISCUSSION**

### **Monolayer study.**

Compression isotherms of mixed films have been examined at the following antibiotic lipid molar ratios  $r = 0.005, 0.01, 0.02, 0.03, 0.04, 0.05, 0.06$  and  $0.1$ . Selected examples of the  $\pi$ -A curves are shown in Figures 1 and 2 together with the compression isotherm of pure DPPC.

As seen from these curves, the presence of the two antibiotics results in modifications of the physical state of the monolayer which are dependent on the concentration.

In both cases, within a certain range of surface pressure, the compression isotherms of the mixture are situated above the one of pure DPPC which means that the films become more resistant and that for a given surface pressure, the molecular area becomes larger. However, the two antibiotics evidence considerable difference:

- for LAS-Na (Figure 1), a more rigid film is maintained up to 35-40 mNm<sup>-1</sup> where the isotherm joins that of pure DPPC and where LAS-Na is likely expelled from the monolayer,

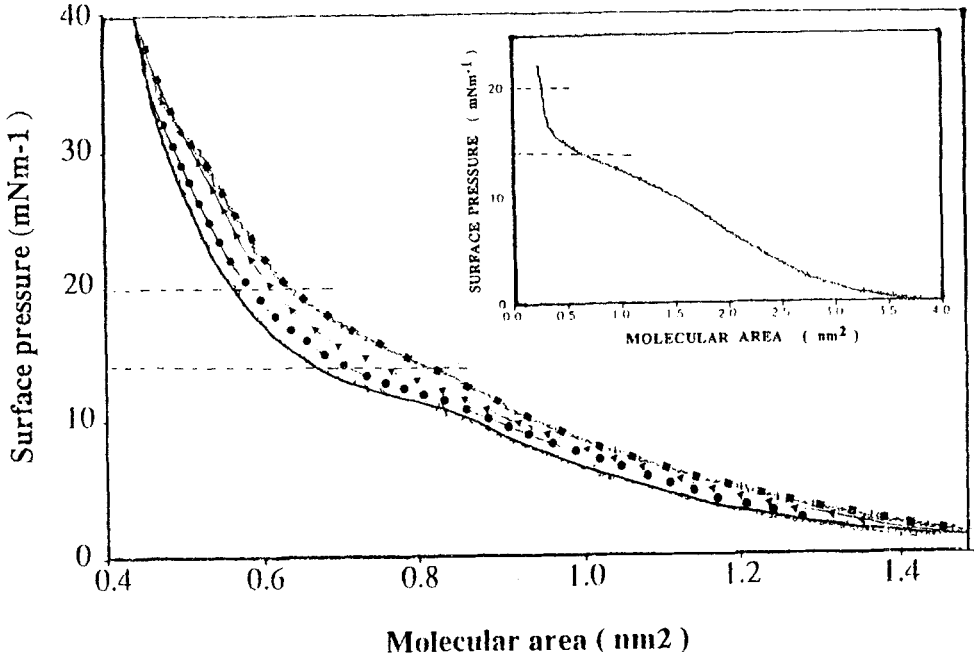


Figure 1. Compression isotherms at 22°C on buffer Hepes 10 mM, NaCl 145 mM, pH 7.4. — Pure DPPC, ●—● LAS-Na+DPPC  $r=0.01$ , ▲—▲ LAS-Na+DPPC  $r=0.04$ , ■—■ LAS-Na+DPPC  $r=0.1$ . Inserted: Compression isotherm under the same conditions of pure LAS-Na.

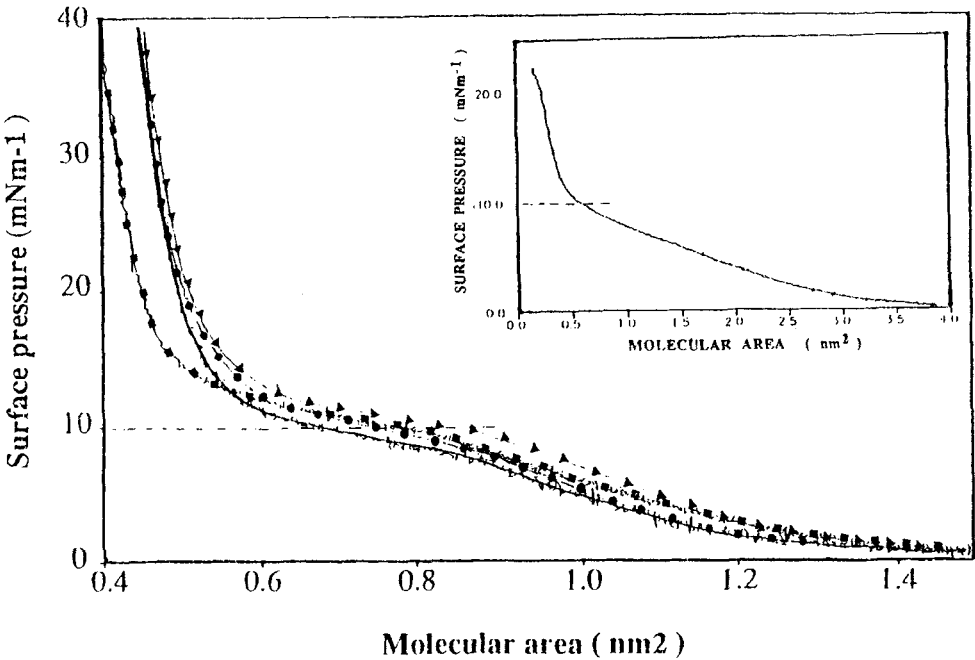


Figure 2. Compression isotherms at 22°C on buffer Hepes 10 mM, NaCl 145 mM, pH 7.4. — Pure DPPC, ●—● MON-Na+DPPC  $r=0.01$ , ▲—▲ MON-Na+DPPC  $r=0.06$ , ■—■ MON-Na+DPPC  $r=0.1$ . Inserted: Compression isotherm under the same conditions of pure MON-Na.

- for MON-Na (Figure 2), the monolayer shows increased rigidity only up to 15 - 20 mNm<sup>-1</sup>. However, this effect diminishes at the highest value  $r = 0.1$  probably with simultaneous expulsion of lipid molecules since the molecular areas become lower for the mixed film than for the film of pure DPPC in the highest pressure range.

We have chosen to express quantitatively the observed effect as the area contribution of each antibiotic molecule  $S_A^*$  to the total molecular area of the mixed films.

The films of the mixtures have been compared with that of pure lipid at a given pressure at which the films undergo the same physical strain. We have, nevertheless, selected surface pressures for which the two films are in the same physical state. The area  $S_A^*$  occupied by the antibiotic molecule in the film can be expressed as :

$$S_A^* = S_{LA} \left(1 + \frac{N_L}{N_A}\right) - \frac{S_L N_L}{N_A} = S_{LA} \left(1 + \frac{1}{r}\right) - \frac{S_L}{r}$$

where  $N_L$  and  $N_A$  are the numbers of moles of lipid and antibiotic respectively in the spreading mixture,  $S_L$  and  $S_{LA}$  are the molecular areas of lipid and lipid/antibiotic mixture (mean value) respectively, obtained from the compression isotherms at a fixed value of the surface pressure, and  $r = N_A/N_L$ . In this way the  $S_A^*$  values are expressed in regions where the molecular area increases are the most important as seen from the  $\pi$ -A compression isotherms in Figures 1 and 2. Figures 3 and 4 show plots of  $S_A^*$  versus  $r$  for LAS-Na and for MON-Na respectively.

In the case of LAS-Na, two pressure levels, 14 and 20 mNm<sup>-1</sup>, have been selected for comparison purposes since observed effect remains up to high surface pressures. For MON-Na, only one pressure level of 10 mNm<sup>-1</sup> has been chosen.

The maximum values of  $S_A^*$  which are exceptionally high, are obtained at the lowest antibiotic concentrations ( $r < 0.02$ ). Both curves show that  $S_A^*$  diminishes as the antibiotic molar ratio increases. The same trend was observed for the LAS-Na/DPPC mixed monolayer on a subphase of pure water where a linear decrease was found <sup>12</sup>.

In order to express the meaning of  $S_A^*$  differently, the ratio  $S_A^*/S_A$  has been determined where  $S_A$  is the molecular area obtained from the compression isotherms of the pure antibiotics (Figures 1 and 2 insert). These curves are completely reproducible when obtained under the same conditions as the compression isotherms of the mixed films and they provide examples of Langmuir films from non classical amphiphiles <sup>14</sup>.

The ratios  $S_A^*/S_A$  are given in Table I at the selected surface pressures for different values of the molar ratio  $r$ .

As seen from the table, the area occupied by the antibiotic molecule in the mixed film is, in all cases, superior to the molecular area of the pure antibiotic. At the pressure of maximum area expansion (i.e. 14 mNm<sup>-1</sup> for LAS-Na and 10 mNm<sup>-1</sup> for MON-Na) at

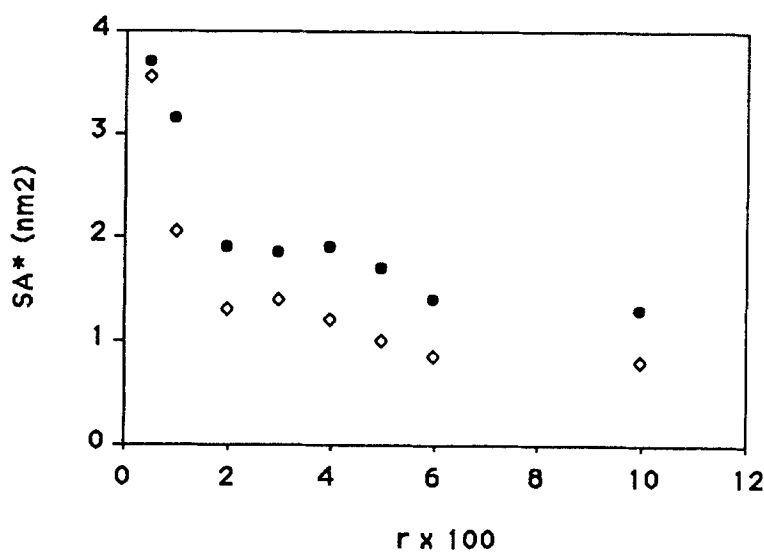


FIGURE 3. Variation of the molecular area  $SA^*$  occupied by LAS-Na in the mixed DPPC film with varying molar ratios  $r$ ,  $\bullet$  at  $14 \text{ mNm}^{-1}$ ,  $\diamond$  at  $20 \text{ mNm}^{-1}$ .

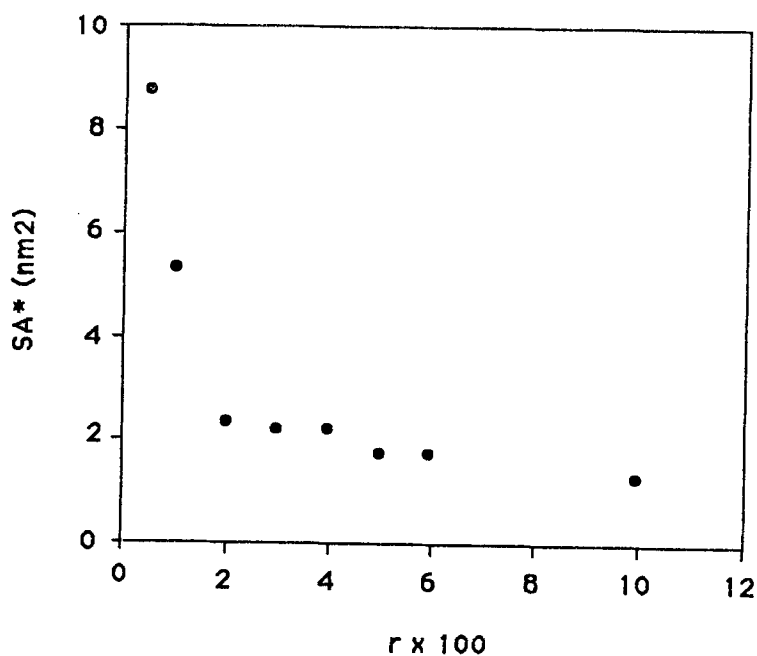


FIGURE 4. Variation of the molecular area  $SA^*$  occupied by MON-Na in the mixed DPPC film with varying molar ratios  $r$  at  $10 \text{ mNm}^{-1}$ .

TABLE I.  $S_A^*/S_A$  ratios versus  $r$  at selected surface pressures.

Antibiotic molecule	$S_A$ nm <sup>2</sup>	Surface pressure mNm <sup>-1</sup>	$r = \text{antibiotic/DPPC (mole/mole)}$							
			0.005	0.01	0.02	0.03	0.04	0.05	0.06	0.1
MON-Na	0.60	10	14.7	8.8	3.9	3.7	3.7	2.9	3.0	2.1
LAS-Na	0.65	14	5.7	4.9	2.9	2.8	3.0	2.6	2.2	2.1
LAS-Na	0.28	20	12.7	7.4	4.7	4.9	4.3	3.5	3.2	2.8

which the two antibiotics have similar  $S_A$  values (about 0.6 nm<sup>2</sup>), MON-Na takes up more space at the interface, this effect being amplified at the lower values of  $r$ . The  $S_A^*/S_A$  ratios for LAS-Na at 20 mNm<sup>-1</sup> show the same tendency as at 14 mNm<sup>-1</sup>, but the  $S_A$  value of 0.28 might be subject to discussion due to limiting conditions of the measurement device.

#### Multilayer study.

Figure 5 shows the DSC profiles recorded during the thermotropic gel to liquid crystal transition of pure DPPC and antibiotic/DPPC mixtures containing increasing concentrations of ionophore. The analysis was performed in excess of water at a constant DPPC concentration (75 mM). Among the six concentrations of LAS-Na and MON-Na studied, four are presented as above.

The DSC curve of pure DPPC depicts the classical recording of the transitions corresponding to lamellar  $L\beta' \rightleftharpoons P\beta'$  \* (34.1°C, pretransition) and  $P\beta' \rightleftharpoons L\alpha$  (41.8°C, main transition) structural changes. The  $L\alpha$  structure has a lamellar bilayer organization with the hydrocarbon chains in all-trans conformation and tilted with respect to the planar bilayer. The pretransition is associated with a structural transformation from a monodimensional lamellar to a bidimensional monoclinic lattice consisting of a lipid lamellae distorted by a

\* The nomenclature  $L\beta'$ ,  $P\beta'$  and  $L\alpha$  is that of Tardieu et al.<sup>15</sup>.



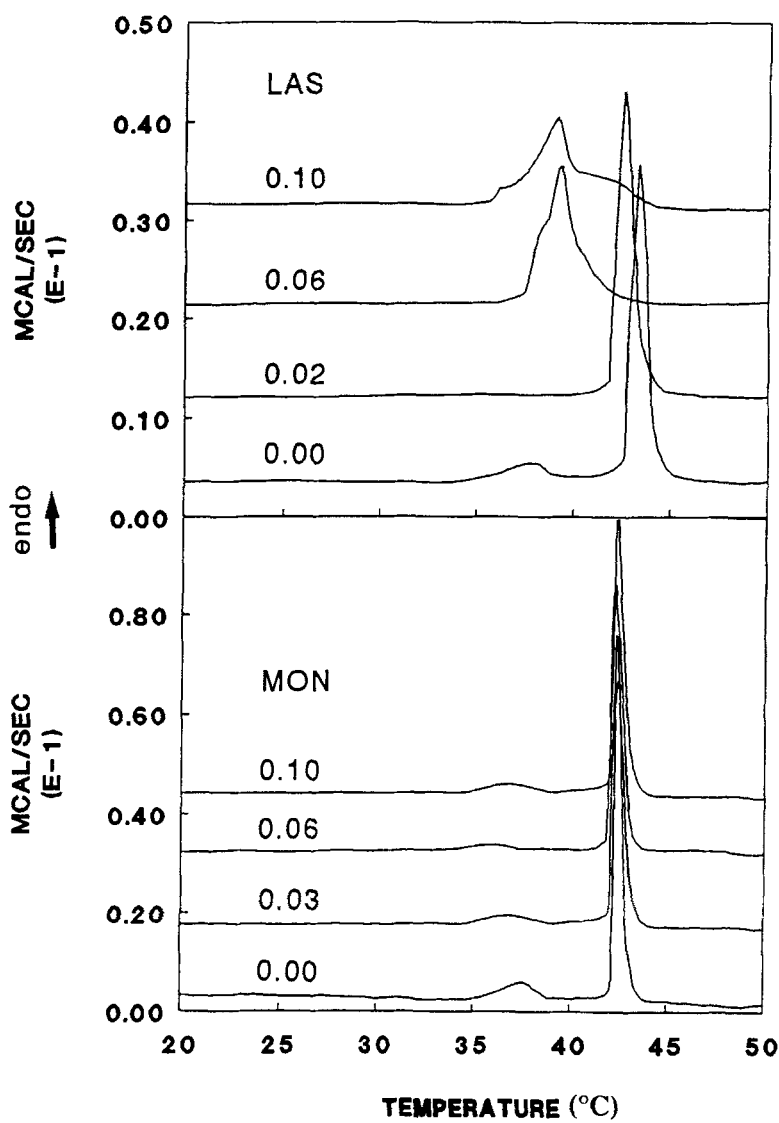


FIGURE 5. DSC curves of DPPC and of mixtures with both antibiotics at different molar ratios  $r$ . Same buffer as in Figure 1, sample weight about 10mg, scanning rate  $4^{\circ} \text{ min}^{-1}$ . Upper part: LAS-Na, lower part: MON-Na.

periodic ripple while the hydrocarbon chains are packed in a regular hexagonal lattice. In the  $L_\alpha$  phase, the lipid chains adopt a disordered state with an average orientation perpendicular to the bilayer plane<sup>16,17</sup>.

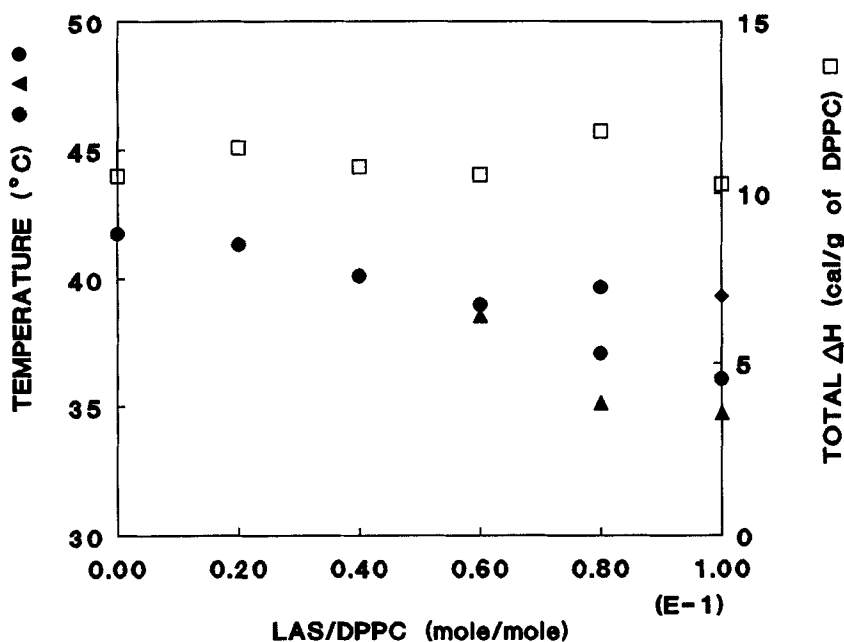


FIGURE 6. Variations of the gel-liquid crystal phase characteristics with varying molar ratios  $r$  for LAS-Na, of the transition onset temperature (filled signs  $\bullet$   $\blacktriangle$   $\blacklozenge$ ) and of the total transition enthalpy (open squares  $\square$ ).

#### - Lasalocid

As shown in Figure 5 (upper part), the profile of the thermotropic transition is modified with increasing proportion of LAS-Na in agreement with a previous calorimetric study<sup>18</sup>. The evolution of the transition parameters versus the LAS- Na/DPPC molar ratios is reported on Figure 6.

The presence of LAS-Na produces vanishing of the pretransition even for  $r$  as low as 0.005. Until  $r = 0.04$ , the main transition is detected as a single peak. However a slight decrease in the temperature and a broadening of the transition is observed, indicating a

decrease in the transition cooperativity and therefore the existence of small perturbations in the DPPC acyl chain organization. Above  $r = 0.04$ , a new peak is observed at a temperature lower than that of the main transition of the pure DPPC and from  $r = 0.08$  a shoulder appears above the main transition (Figure 5 upper part and Figure 6).

The occurrence of DSC peaks distinct from that of the main transition shows that increasing LAS-Na concentration provoke a pronounced disorganization of DPPC chains and may indicate specific interactions between LAS-Na and part of DPPC molecules. This might induce lateral phase separation in the phospholipid membrane. The existence of binding sites of LAS-Na to DPPC multibilayers has been evidenced by Aranda and Gomez<sup>18</sup> from fluorescence measurements.

Despite the drastic modifications observed through the thermotropic transition, the total enthalpy does not change whatever  $r$  (Figure 6). This indicates that all DPPC molecules, in interaction with LAS-Na or not, participate in the main transition. However, the shifting of the temperature and the existence of several peaks ( $r > 0.04$ ) suggest that the chain melting occurs via successive steps according to their packing characteristics in the bilayer.

#### *-Monensin*

The DSC curves recorded for DPPC/MON-Na mixtures (Figure 5 lower part) appear for all ratios very similar to that of pure DPPC. The pretransition is clearly detected even for  $r=0.1$ , although its amplitude progressively decreases. The cooperativity of the main transition is perfectly preserved. This thermal behavior evidences that, at least in the antibiotic concentration range examined, the structural arrangement of DPPC acyl chains in the  $L\beta'$ ,  $P\beta'$  and  $L\alpha$  is not perturbed by the presence of MON-Na.

Jain and Wu<sup>19</sup> have related the effect induced by an additive on the DPPC phase transition profile to the localization of this additive along the thickness of the bilayer. The DSC profile arises from the change in the organization of acyl chains and then represents a description of the phase properties of the lipid bilayer as modified by various additives. The shape of the transition profile is indicative of the type of perturbation. Different types of perturbations have been found which globally depend on the polarity of the compounds, this last determining the localization in the bilayer. According to this qualitative classification, the ionophores of the Nigericin group have been localized close to the glycerol backbone of DPPC. However, as LAS-Na and MON-Na do not induce the same effect on the phase transition behavior, their interaction with DPPC molecules even if it might concern the polar head group, implies a different nature. A better understanding of the interaction modes of these ionophores in the model membrane needs contribution of other physical methods.

## **CONCLUSION**

The two investigation techniques show that different effects arise from LAS-Na and MON-Na addition to the phospholipid in monolayers as well as in bilayers and that the most singular behavior is produced by MON-Na.

In monolayers, the main effect resulting from antibiotic addition is to increase the film resistance, which is produced by MON-Na within a limited surface pressure whereas LAS-Na renders the film more pressure resistant over a much larger pressure interval. Concerning the concentration dependence, the lower the antibiotic ratio, the greater the effect of each molecule.

LAS-Na strongly perturbs the phospholipid phase transition, abolishing the pretransition, and inducing, up to three steps for the chain melting in the main transition. In contrast, MON-Na does not show any significant effect on the phospholipid phase transition even for high concentrations.

Although the molecules LAS-Na and MON-Na belong to the same group of antibiotic ionophores, our study shows that they have different implantation modes at least in model membranes.

**Acknowledgement.** This work was supported by DRET ( DGA ).

## **REFERENCES**

1. W.F. Nijenhuis, J.J.B. Walhof, E.J.R. Sudhölter and D.N. Reinhoudt, Recl. Trav. Chim. Pays-Bas, **110**, 265-270 (1991).
2. Y.Habata, K. Uchida, Y. Sato and S. Akabori, J. Memb. Sci., **85**, 175-181 (1993).
3. H.H. Mollenhauer, D.J. Morré and L.D. Rowe, Biochim. Biophys. Acta, **1031**, 225-246 (1990).
4. G.R. Painter, R. Pollack and B.C. Pressman, Biochemistry, **21**, 5613-5620 (1982)
5. B.C. Pressman, E.J. Harris, W.S. Jagger and J.H. Johnson, Biochemistry, **58**, 1949-1955 (1967).
6. E.L. Cussler, AIChE Journ., **17**, 1300-1303 (1971).
7. Y.N. Antonenko and L.S. Yaguzhinsky, Biochim. Biophys. Acta, **938**, 125-130 (1988).

8. F.G. Riddel, S. Arumugam and B.G. Cox, Biochim. Biophys. Acta, **944**, 279-284 (1988).
9. M.N. Borrel, E.Pereira, M. Fiallo and A. Garnier-Suillerot, European Science Foundation (ESF) Wroclaw-Karpacz, Poland, September 1993.
10. Y. Pointud, J. Julliard, G.Jeminet and L.David, J. Chem. Soc., Faraday Trans.,1, **77**, 1-8 (1981).
11. A.Hochapfel, H. Hasmonay, M. Jaffrain and P.Peretti, Mol. Cryst. Liq. Cryst., **215**, 221-228 (1992).
12. H. Hasmonay, A. Hochapfel, C. Betrencourt, A. Tahir and P.Peretti, Biochim. Biophys. Acta (1994) in press.
13. C. Grabielle - Madelmont and R. Perron, J. Colloid Interface Sci., **95**, 471-493 (1983).
14. A. Hochapfel, H. Hasmonay, M. Jaffrain and P. Peretti, Thin Solid Films, **221**, 292-297 (1992).
15. A. Tardieu, V. Luzzati and C. Reman, J. Mol. Biol., **75**, 711 (1973).
16. M. J. Janiak, D. M. Small and G. G. Shipley, J. Biol. Chem., **254**, 6068-6078 (1979).
17. M. J. Ruocco and G.G. Shipley, Biochim. Biophys. Acta, **691**, 309-320 (1982).
18. X. F.J. Aranda and J.C. Gomez-Fernandez, Biochim. Biophys. Acta, **860**, 125-130 (1986).
19. M. K. Jain and N. M. Wu, J.Membrane Biol, **34**, 157-201 (1977).